

## THE IMAGING OF GDANSK BAY SEABED BY USING SIDE SONAR

Grażyna Grelowska<sup>1</sup>

Eugeniusz Kozaczka<sup>1,2</sup>

Dominika Witos-Okrasińska<sup>1</sup>

Wojciech Szymczak<sup>2</sup>

<sup>1</sup> Gdańsk University of Technology, Poland

<sup>2</sup> Polish Naval Academy, Gdynia, Poland

### ABSTRACT

*This paper is mainly aimed at presentation of an impact of environmental conditions on imaging accuracy by using hydro-acoustic systems in waters of a high non-uniformity of spatial distribution of hydrological parameters. Impact of refraction on erroneous estimation of range, in case of wave radiation into water under a large angle, like in side sonars or multi-beam echo-sounders, is especially important. In this paper seasonal changes in sound speed and its impact on acoustic beam refraction is discussed. And, examples which illustrate errors in determination of side sonar range occurred during last investigations carried out in Gdansk Bay waters are presented.*

**Keywords:**

### INTRODUCTION

Side sonar is a device which makes imaging a relatively large area of seabed with high resolution, possible. A solution proposed by Prof. H. Edgerton<sup>1</sup> in 1960 to be used in side sonar has served initially to search for submarines and other objects on seabed. Further investigations led to development of this technology into direction of sea geophysics and geology<sup>2,3,4,5</sup>. Contemporary hydro-acoustic systems including also side sonars are implemented in systems for seabed exploration and find many other applications such as e.g.:

- investigations on seabed morphology and sediment characteristics (e.g. occurrence of reliefs, depressions, sediment structures etc)<sup>6,7,8</sup>,

- working out maps of distributions of seabed sediments and – in special cases – even bio-ceonosis, e.g. sea grass meadows<sup>9</sup>,
- detection of special targets on seabed such as ship wrecks, mines, drown objects<sup>10</sup>,
- identification of suitable locations for offshore infrastructures (drilling platforms, pipelines, cables etc)<sup>11</sup>,
- seabed monitoring for environment management purposes.

In view of frequencies of acoustic waves radiated to water, sonars are divided into two kinds: of low-frequency (up to 100 kHz) and high-frequency (over 100 kHz up to 1 MHz)<sup>12</sup>. Imaging accuracy increases along with frequency increasing. Observation range of sonars depends on their frequency and for high-frequency sonars it amounts to about 100 m in view

of damping rise proportionally to the square of frequency. At larger depth of water area an often used solution is to tow an immersed sonar behind a floating unit that makes it possible to achieve a distance required between sonar's antenna and seabed.

Side sonar's resolution may be understood in two ways:

- as system's resolution defined by a form of acoustic beam and pulse length<sup>3</sup>, or
- as image resolution defined by number of pixels.

The system's resolution depends on spatial distribution of acoustic power which decides on dimensions of the so called footprint. Transverse resolution and range resolution of sonar was described by Jones<sup>3</sup>. It may be meant as a resolution across-track footprint and resolution along-track footprint<sup>5</sup>. The system's resolution depends on a form and kind of transmitting converter. The transverse resolution is also affected by motion speed of sonar's converter in relation to seabed. Horizontal beam breadth amounts to less than 1° for 1 000 kHz frequency and about 1-2° for frequencies ranging from 100 to 200 kHz. Vertical beam breadth – for different types of side sonars – ranges from 30 to 75°. Therefore, depending on a type of sonar, the resolution growing with water depth, is equal to about 1 cm (in case of transverse one) up to a few cm (of range one).

The resolution is not the only parameter which decides on accuracy and quality of mapping. Environmental factors such as spatial distributions of water temperature, salinity and density which decide on spatial distribution of sound speed and consequently on acoustic beam refraction, play here an important role. Also course and speed of sonar's antenna relative to seabed, antenna's heel, distance over the bottom and operation range settings are the elements on which quality of sonar's data depends. The factors may significantly influence the mapping.

Considerations presented in this paper deal with an impact of environmental conditions, especially sound speed distribution on mapping accuracy of underwater images, which is exemplified by results of measurements conducted in the area of Gdansk Deep.

## CHANGES IN HYDROLOGICAL CONDITIONS OF GDANSK BAY

The Baltic Sea is characteristic of yearly changeable hydrological conditions which influence hydro-acoustic conditions of the water area<sup>13,14,15,16,17</sup>. A characteristic feature of Baltic Sea waters is their stratification. Three water layers: upper layer, deep layer and intermediate layer are distinguished – Fig. 1. In vertical distribution of salinity the intermediate layer – halocline is characteristic of a sudden change in salinity and occurs, depending on a Baltic Sea region, beginning from the depth of 40 up to 60 m or 60 up to 80 m. In vertical distribution of seasonal temperature a water layer characteristic of a sudden change in temperature – thermo-cline appears in spring and summer months. Surface waters are of a low salinity and their temperature depends on a season of the year. Also a strong influence of wind

(the so called wind mixing) on changes in distribution of hydrological parameters is observed. Deep waters have much greater salinity and small temperature variation, and, in contrast to typical shallow seas, in the Baltic Sea deep water temperature increases towards bottom. This results from the fact that irregular episodes of the pouring-in of salt water from the North Sea affect water temperature and salinity of that part of the Baltic Sea.

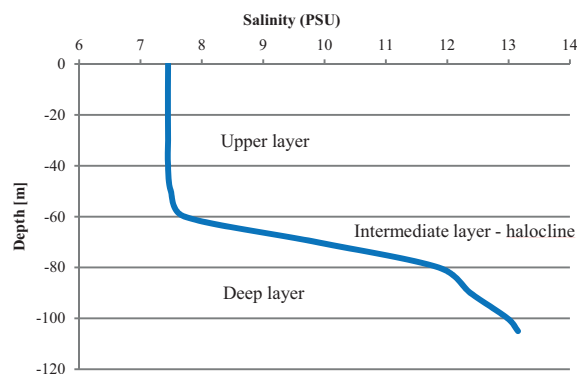


Fig. 1. Stratification of Baltic Sea water

Characteristic features of South Baltic Sea's waters are illustrated in Fig. 2 and 3. They present average values of temperature and salinity in particular month of the year, based on the data collected in the years 2000-2010 for the Gdansk Deep region.

The largest temperature changes are observed in the upper layer – Fig. 2. It is associated with heat exchange through water-atmosphere boundary. The highest temperature is reached in summer months (August, September), the lowest – in winter months (February, March).

In hydrological conditions typical for the South Baltic Sea sound speed changes are most affected by temperature changes. The highest value of sound speed is reached close to water surface in summer month. A characteristic feature of Baltic Sea water is that minimum value of sound speed occurs in the intermediate layer, then it increases towards seabed. The distribution is analogous to that of temperature. As a matter of fact in the Baltic Sea no seasonal changes in salinity are observed. Its lowest value is reached in the upper layer, the highest – in the deep layer. Vertical distribution of salinity in the Baltic Sea changes along with growing distance from Danish Straits. The greater the distance the smaller the salinity. Changes observed in distributions of instantaneous hydrologic and hydro-acoustic parameters result from local phenomena such as vortices, wind mixing, water inflow from big rivers or upwelling\*.

\* Lifting deep cold water onto surface.

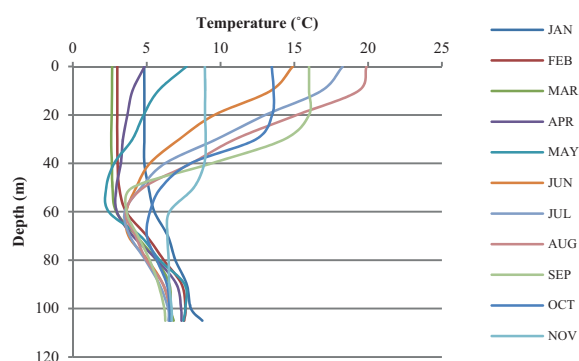


Fig. 2. Vertical distribution of temperature

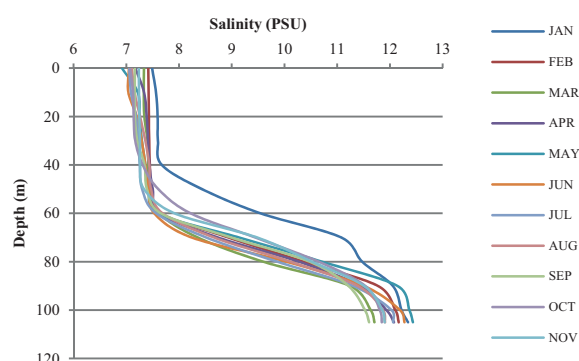


Fig. 3. Vertical distribution of salinity

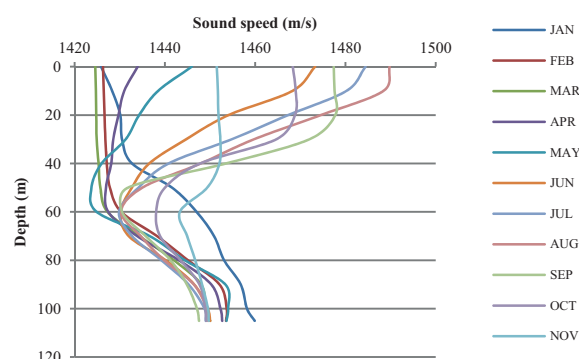


Fig. 4. Vertical distribution of sound speed

The change of sound speed in function of depth results in that refraction phenomenon is of a great importance in case of devices which use acoustic waves for information transmitting. Refraction affects accuracy in location of objects when acoustic wave is radiated into water under an angle. In hydro-acoustic devices sound speed value is most often assumed constant in function of depth. The fact of changeable sound speed in function of depth is not taken at all into account. In subsequent diagrams a difference in path of acoustic wave beam radiated into water under 60° angle in different seasons of the year, is presented. For the calculations the real instantaneous distributions recorded in February, August and November were selected (Fig. 5). The results were then compared with the range determined

under the condition of no vertical sound speed gradient:  $dc/dh=0$ .

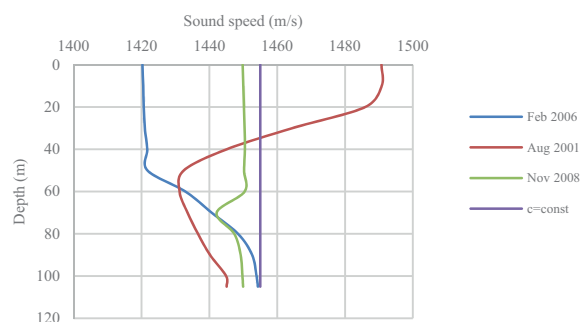


Fig. 5. Example sound speed distributions recorded in Gdansk Deep region in February, August and November and the constant distribution assumed for calculations.

Use was made of a refraction theory adapted from optics, i.e. change in wave propagation during passing into a medium of another sound speed. Water column was divided into horizontal layers to each of them constant sound speed values were assigned. In accordance with Snell law<sup>18</sup> wave diffraction on the boundary of layers with different sound speeds is described by the following relation:

$$\frac{\sin \beta_1}{c_1} = \frac{\sin \beta_2}{c_2} = \text{const.}$$

where:  $c_1$ ,  $c_2$  – stand for sound speed in subsequent layers,  $\beta_1$  – beam angle of incidence on the boundary of layers, and  $\beta_2$  – beam angle of penetration into second layer. The same procedure is used for boundaries of all layers in water column (Fig. 6).

In carrying out the calculations, information about vertical sound speed distribution achieved from a given measurement point is used. In propagating the wave directed under an angle the point of passing the beam through the boundary of subsequent layers is shifted in horizontal plane against the point in which the measurement has been made. As results from the calculations, differences in ranges are not greater than 20 m. In the present stage of this research it was assumed that the values of vertical sound speed distribution measured in the point represent spatial sound speed distribution in water column of such radius. A detail assessment of refraction influence on error in estimation of hydro-acoustic device range would require an information about spatial distribution of sound speed. However, to execute such tests in sea conditions is a very difficult task.

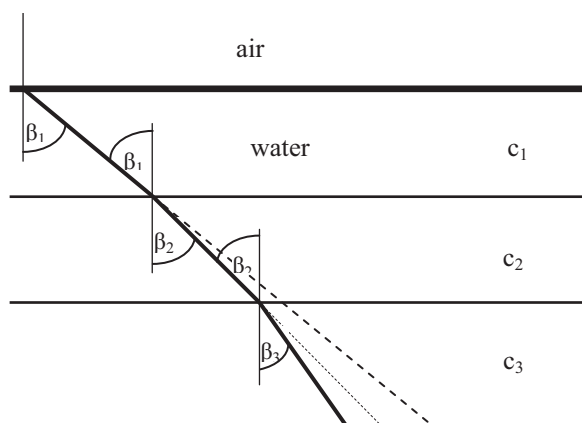


Fig. 6. Odd refraction of acoustic beam during its passing through boundary of layers of different sound speed:  $c_1 > c_2 > c_3$ ,  $\beta_3 < \beta_2 < \beta_1$

Acoustic wave which propagates into a medium with the sound speed  $c_1$  falls onto boundary of media under the angle  $\beta_1$  counted against normal to the boundary. After passing into a medium of another sound speed the beam penetration angle changes to  $\beta_2$ . This causes beam deflection and non-linear trajectory forming, that consequently results in an error in determination of position of objects detected by hydro-location devices.

Subsequent diagrams show range differences determined for the sound speed distributions given in Fig. 5 under assumption that acoustic beam is directed to water under  $60^\circ$  angle.

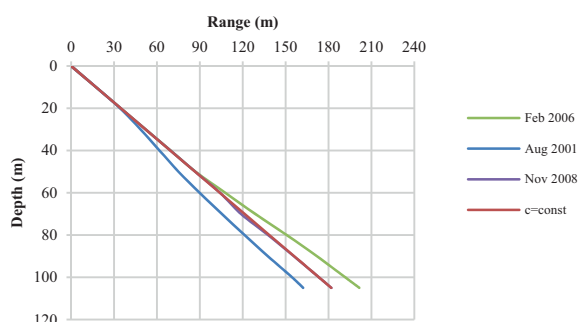


Fig. 7. Trajectory of acoustic beam directed to water given for different months under assumption that sound speed distribution is uniform.

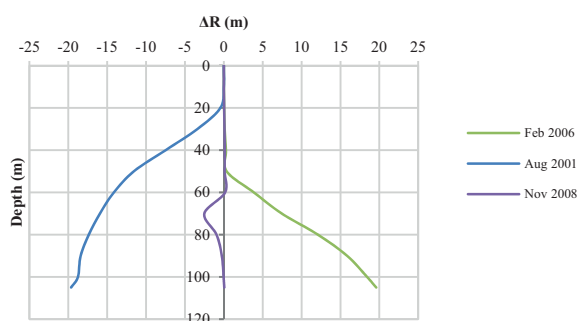


Fig. 8. Error in range determination for the sound speed distributions given in Fig. 5

Depending on a sound speed distribution, differences between real range and its value in a homogenous medium are achieved. If a distribution is close to linear the differences are rather small. It may be illustrated by the distribution taken in November 2008. In this case the range coincides practically with that calculated for homogenous medium. Comparing the errors in range determination conducted in summer and winter months one can observe that the difference between the points of reaching the bottom in the depth of abt. 100 m by acoustic beam comes even to 40 m, Fig. 8.

## MEASURING SYSTEM

The measuring system was installed on s/y Freija, a 12 m research boat, Fig. 9. The boat is equipped a.o. with a module of Simrad Structure Scan side sonar cooperating with Simrad NSS9-evo2 plotter – a sending-receiving module. The system, apart from recording sonar images, makes automation of measurements along given cross-sections possible for its operator by using an autopilot integrated with the system. The positioning of research boat on navigation charts is ensured by 12-channel GPS receiver equipped with Garmin GPS 17x location sensor – this way the system's accuracy is ensured to be 3 m. Safety of conducting the investigations is provided by gaining information from AIS system and radar. The side sonar converter was fastened on boat's bottom by means of a special holder. Place of installation of the converter was selected at 3,5 m distance from the stern in order to eliminate influence of disturbances generated by screw propeller and aerated water flowing around the keel. Additionally, the selected place is characteristic of small rolling and pitching motions, otherwise it could affect quality of obtained acoustic images. The maximum range of the system reaches 183 m, maximum sounding depth – 92 m. Acoustic wave radiation frequency is equal to 455 kHz.



Fig. 9. The research boat – s/y Freija

The measurements were performed in Gdansk Bay region in August and September 2016 and June 2017. During recording



seabed images the boat was moving with 2 knot speed. Several series of measurements were made in different points and different depths. The recording is carried out continuously and the data are imaged live on the sounder plotter (Fig. 10) installed inside the boat. The data are additionally recorded on an external storage medium.

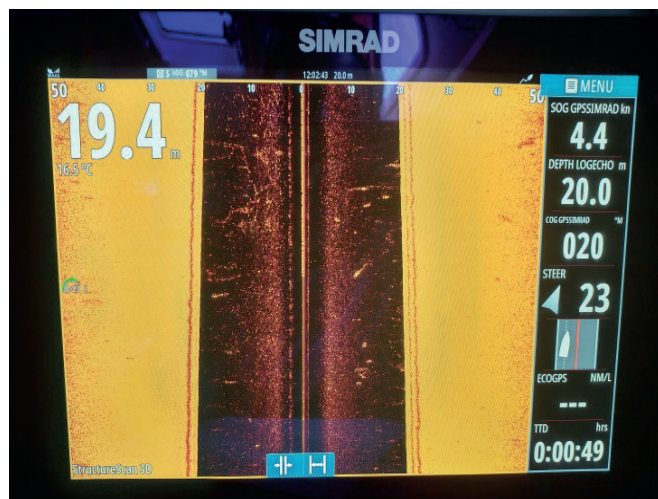


Fig. 10. Plotter

Sound speed measurements were conducted by means of a CastAway CTD compact sounder which allows for fast measuring sound speed. Both the side sonar and CTD sounder are integrated with the GPS receiver, that facilitates to make catalogues of gained profiles by assigning them automatically to particular fragments of an investigated water area.

In comparison with the commonly used measuring modules, transmission of the data recorded in internal memory of the device is possible through an internal Bluetooth module (Fig. 11), i.e. without necessity of connecting any external cables. The sounder allows to take profiles in the depth up to 100 m. Based on the water depth measurements, sound speed value is determined with the use of Chen-Millero empirical formula<sup>19</sup>. The established measuring accuracy is as follows: for salinity – 0,01 PSU, for depth – 0,01 m, for temperature – 0,05 °C, for sampling frequency – 5 Hz.

The device is fitted with a 6-core conductometric sensor connected to a fast-reacting thermistor whose response amounts to less than 200 ms, that allows to reach a high measuring accuracy at high resolution. The sounder is lowered onto seabed due to its own weight; its resolution varies within the range from 0,15 to 0,53 m, depending on lowering speed.



Fig. 11. Sonic sounder for measuring sound speed

## RESULTS OF THE MEASUREMENTS

During the performed investigations, images of fragments of Gdansk Bay seabed were achieved together with information on conditions of acoustic wave propagation prevailing in the time of the tests. Recording the images was carried out continuously. Points where sound speed was measured are shown on the chart (Fig. 12).

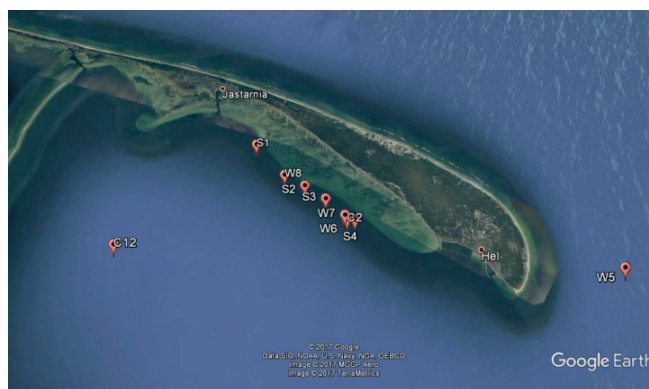


Fig. 12. The chart with marked points where sound speed was measured

Fig. 13 presents a fragment of a signal recorded by the side sonar. 1400 samples per each boat's side were recorded in each sounding operation irrespective of a selected observation range. For instance at the selected range of 80 m the sampling interval is equivalent to the distance of about  $5.7 \times 10^{-2}$  m.

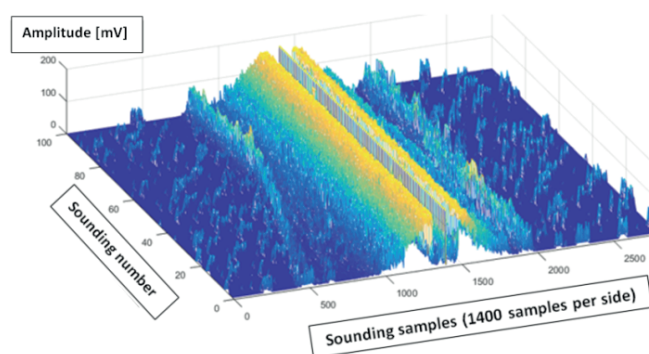


Fig. 13. A signal recorded by side sonar

The signal is transformed into the form of images visible on the plotter. Fig.14 shows the seabed image recorded close to the point W7 in September 2016.

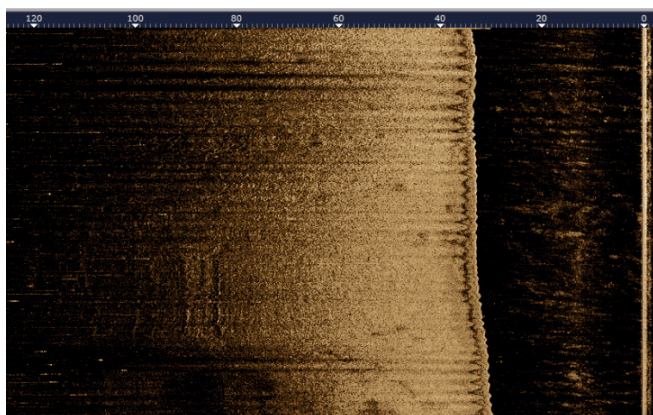


Fig. 14. Seabed image recorded close to the point W7

The wave propagation conditions in September in the investigated region are described by the acoustic wave speed distributions shown in Fig. 15.

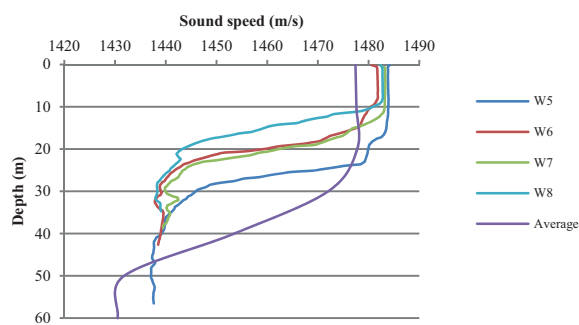


Fig. 15. Vertical sound speed distributions taken in the selected stations in September 2016.

Comparing these distributions with the curve which illustrates a distribution typical for September, determined on the basis of results from the years 2000-2010, it is possible to observe higher sound speed values in the upper layer and a more sudden drop of the speed at the relatively small depth of 23,59 m. It results from occurrence of a higher temperature (17,5°C) in the subsurface stirred-water layer of about 23 m in thickness (Fig. 16). Under the warm water layer a cold water mass was present. In the depth of 30 m the water had temperature of 7,21°C whereas such temperature was usually observed about 15 m deeper. The sharply marked thermocline resulted in a sudden change in sound speed.

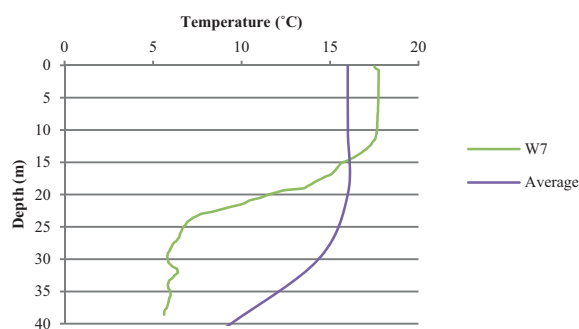


Fig. 16. Water temperature changes in the station W5 in September 2016 and averaged respective data from the years 2000-2010

This anomaly in temperature distribution caused a significant odd refraction. The curves in Fig. 17 show an area covered by side sonar beam in natural conditions compared with the area determined under assumption that sound speed is distributed uniformly within the whole water column. At 38 m depth the beam refraction causes that points on the echo-sounder screen are depicted in the distance of over 100 m from the boat's path whereas they are really located in the distance only a little greater than 80 m.

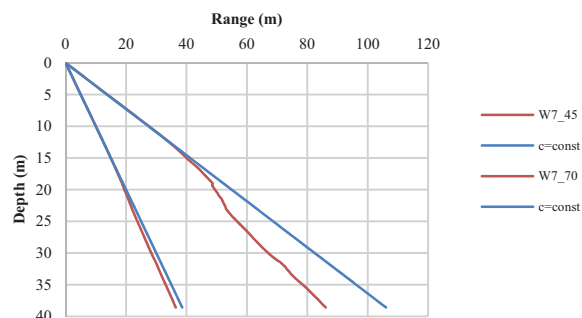


Fig. 17. Side sonar theoretical range versus real one in the station W7

The next figure presents an error in range determination resulting from refraction. At the bottom it amounted to 2,14 m for side sonar internal beam and 19,92 m for its external beam.

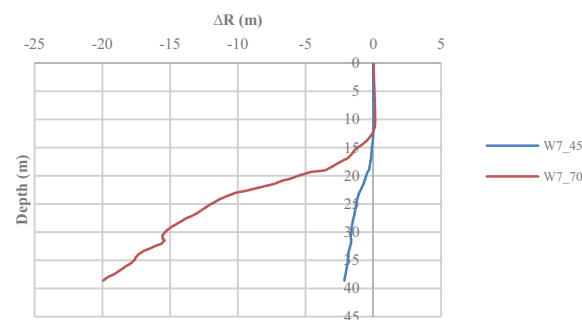


Fig. 18. Range determination error in the station W7 for the acoustic beams directed under the angles of 45° and 70°

Seabed investigations are often aimed at searching objects lying on seabed. Fig. 19 shows the wreck of the ship „Delfin” drowned in the middle of Puck Bay (Point C12).



Fig. 19. The wreck of the ship „Delfin” – the image from the point C12

Fig. 20 shows the sound speed distribution taken in the point C12 in June 2017.

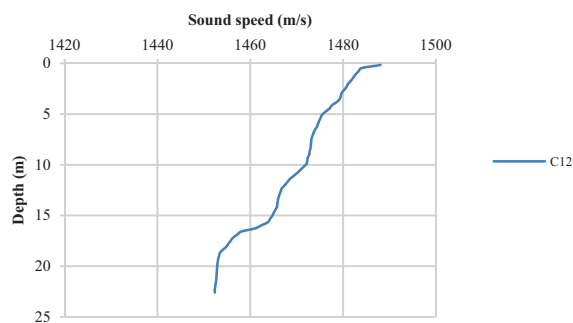


Fig. 20. The sound speed distribution taken in the point C12 in June 2017

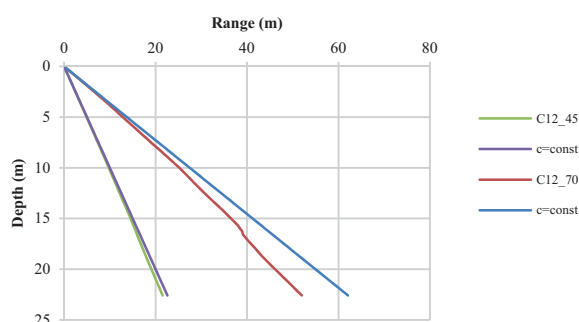


Fig. 21. Side sonar theoretical range versus real one in the station C12

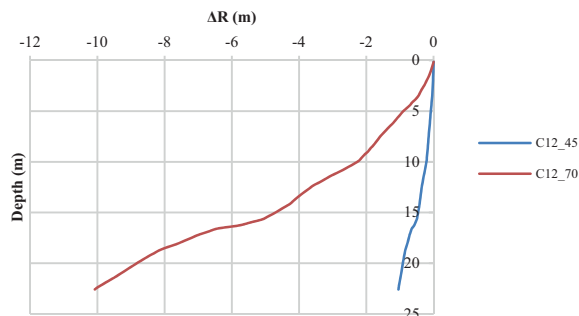


Fig. 22. Range determination error in the station C12 for the acoustic beams directed under the angles of 45° and 70°

Also in this case the odd refraction causes error in range determination in conditions of large beam penetration angles.

## SUMMARY

Environmental conditions in shallow sea, especially changeable seasonal temperature distribution which directly affects spatial distribution of sound speed field, are of a great importance for accuracy in seabed imaging by means of side sonar. Based on the research results presented in this paper it can be stated that error in estimating range of sound wave beam penetrating under a large angle is significant even in case of a not very large depth.

For instance, for external acoustic beam of the sonar used in the presented measurements, penetrating water under 70° angle – the error in the tests carried out on the station C12 of 21 m depth in June 2017 amounted to 10 m, and on the station W7 of 38 m depth in September 2016 – 20 m. The GPS system used for the research boat positioning determined its position with the error of 3 m.

Range estimation errors or imaging accuracy in testing with the use of hydro-acoustic devices depend on many instrumental and environmental factors or those associated with ship motion. The presented results indicate that errors associated with refraction should be taken into account during interpretation of test results.

## ACKNOWLEDGEMENTS

This research project has been partially financed by the Ministry of Science and Higher Education in the frames of funds intended for statutory activity of Gdansk University of Technology and Polish Naval Academy.

## BIBLIOGRAPHY

1. J. P. Fish, H. A. Carr: Sound underwater images-A guide to the generation and interpretation of side scan sonar data. Orleans, MA: Lower Cape Publishing, 1990
2. R.B. Belderson, N.H. Kenyon, A.H. Stride, A.R. Stubbs: Sonographs of the Sea Floor a Picture Atlas. Elsevier, Amsterdam, London, New York, 1972
3. E.J.W. Jones: Marine Geophysics. Wiley, 1999
4. J. Tęgowski: Acoustic classification of sediments (in Polish), Rozprawy i Monografie, 19/2006, PAN Instytut Oceanologii, Sopot, 2006
5. P. Blondel: The Handbook of Side-scan Sonar. Springer Verlag, 2009
6. E. Kozaczka, G. Grelowska, W. Szymczak, S. Kozaczka: The examination of the upper layer of the seabed by means of the acoustic methods, Acta Physica Polonica A, Vol. 119, 6A,, 2011, pp.1091-1094
7. G. Grelowska, E. Kozaczka: Underwater acoustic imaging of the sea, Archives of Acoustics, Vol. 39, 4,, 2014, pp.439-452
8. E. Kozaczka, G. Grelowska, S. Kozaczka: Images of the seabed of the Gulf of Gdansk obtained by means of the parametric sonar, Acta Physica Polonica A, Vol. 118, No 1,, 2010, pp.91-94
9. G. Grelowska, E. Kozaczka, S. Kozaczka, W. Szymczak: Gdansk Bay seabed sounding and classification of its results, Polish Maritime Research No 3 (79) Vol 20,, 2013, pp. 45-50



10. E. Kozaczka, G. Grelowska, S. Kozaczka, W. Szymczak: Detection of objects buried in the sea bottom with the use of parametric echosounder, Archives on Acoustics, 38, 1, 2013, pp. 99-104
11. P. Dymarski, E. Ciba, T. Marcinkowski: Effective method for determining environmental loads on supporting structures for offshore wind turbines. Polish Maritime Research 1(89) Vol. 23, 2016, pp. 52-60
12. A. Savini: Side-Scan Sonar as a Tool for Seafloor Imagery: Examples from the Mediterranean Continental Margin, Sonar Systems, InTech, Available from: <http://www.intechopen.com/books/sonar-systems/side-scan-sonar-as-a-tool-for-seafloor-imageryexamples-from-the-mediterranean-continental-margin>, 2011
13. The BACC Author Team: Second assessment of climate change for the Baltic Sea basin, Springer, 2015
14. G. Grelowska, D. Witos: Acoustic climate of the Gulf of Gdansk in years 2000-2010, Hydroacoustics vol. 19, 2016, pp. 129-138
15. G. Grelowska: Study of seasonal acoustic properties of sea water in selected waters of the Southern Baltic, Polish Maritime Research, V. 23, 1, 2016, pp. 25-30
16. A. Dolecki, G. Grelowska: Oceanographic database – a component of naval operations oceanographic support, Polish Journal of Environmental Studies, Vol. 19, 4A., 2010, pp. 9-14
17. G. Grelowska, E. Kozaczka: The study of acoustic climate of the Southern Baltic, Proc. Mtgs. Acoust. 28, 005001, 2016; doi: 10.1121/2.0000342
18. X. Lurton: An Introduction to Underwater Acoustics – Principles and Applications, 2<sup>nd</sup> Edition, Springer Verlag, Berlin, 2003
19. N.P. Fofonoff and R.C. Millard Jr: Algorithms for computation of fundamental properties of seawater (1983), UNESCO technical papers in marine science. No. 44, Division of Marine Sciences. UNESCO, Place de Fontenoy, 75700 Paris

## CONTACT WITH THE AUTHORS

**Grażyna Grelowska**

**Eugeniusz Kozaczka**

**Dominika Witos-Okraśńska**

*e-mail: dominika.witos@pg.gda.pl*

Gdańsk University of Technology  
Faculty of Ocean Engineering and Ship Technology  
11/12 Narutowicza St.  
80 - 233 Gdańsk  
**POLAND**

**Wojciech Szymczak**

*e-mail: w.szymczak@amw.gdynia.p*

Polish Naval Academy  
69 Śmidowicza St.  
81-127 Gdynia  
**POLAND**